

Article

# Preparation of Metallic Iron Powder from Pyrite Cinder by Carbothermic Reduction and Magnetic Separation

Hongming Long, Tiejun Chun \*, Zhanxia Di, Ping Wang, Qingmin Meng and Jiaxin Li

School of Metallurgical Engineering, Anhui University of Technology, Ma'anshan 243002, China; yaflhm@126.com (H.L.); dzx2012@ahut.edu.cn (Z.D.); wangping63629@163.com (P.W.); mengqingmin@ahut.edu.cn (Q.M.); lijx@ahut.edu.cn (J.L.)

\* Correspondence: springcsu@126.com; Tel.: +86-183-9556-1203

Academic Editor: Corby G. Anderson

Received: 16 February 2016; Accepted: 11 April 2016; Published: 16 April 2016

**Abstract:** The reduction and magnetic separation procedure of pyrite cinder in the presence of a borax additive was performed for the preparation of reduced powder. The effects of borax dosage, reduction temperature, reduction time and grinding fineness were investigated. The results show that when pyrite cinder briquettes with 5% borax were pre-oxidized at 1050 °C for 10 min, and reduced at 1050 °C for 80 min, with the grinding fineness (<0.44 mm) passing 81%, the iron recovery was 91.71% and the iron grade of the magnetic concentrate was 92.98%. In addition, the microstructures of the products were analyzed by optical microscope, scanning electron microscope (SEM), and mineralography, and the products were also studied by the X-ray powder diffraction technique (XRD) to investigate the mechanism; the results show that the borax additive was approved as a good additive to improve the separation of iron and gangue.

**Keywords:** pyrite cinder; carbothermic reduction; magnetic separation; metallic iron powder

## 1. Introduction

Pyrite cinders are produced as a by-product of the sulfuric acid industry, containing  $\text{Fe}_2\text{O}_3$ ,  $\text{Fe}_3\text{O}_4$ , metallic silicate, hazardous heavy metals, *etc.* In China, more than 30% of sulfuric acid is produced from pyrites ores, and more than 10 million tons of pyrite cinders are produced annually, with the total generation of pyrite cinders at over 10 million tons per [1,2]. The storage of pyrite cinder consumes a great deal of land and creates a serious environmental problem [3,4]. Nevertheless, the utilization of pyrite cinders was greatly limited due to its low iron grade and high sulphur content [5].

In the previous research, physical separation processes have been used to separate gangue and iron, including gravity separation, magnetic separation, and floatation [6–8]. However, as the high-temperature procedure alters the physical and chemical properties of pyrite cinder, it was hard to separate the iron and gangue of pyrite cinder by transitional physical methods, and the iron grade of the iron concentrate obtained was also low. In addition, chemical methods [9,10] were also used to treat the pyrite cinder. Nevertheless, the chemical methods have a high cost of reducing reagents which could lead to secondary pollution. Based on the aforementioned introduction, it can be found that a capable method to separate the iron and gangue of the pyrite cinder efficiently is significant for realizing the utilization and preparing the iron concentrate from pyrite cinder.

Therefore, this study will focus on the recovery of the iron and the preparation of reduced powder obtained from pyrite cinder by adopting the reduction-magnetic separation method which has been proved to be an effective way to recover iron from solid wastes [11,12]. The effects of additive dosage, reduction temperature, reduction time and grinding fineness on the iron recovery are investigated.

## 2. Materials and Methods

### 2.1. Raw Material

Table 1 shows the chemical composition of pyrite cinder. The contents of Fe and FeO are 60.95% and 12.61%. The contents of SiO<sub>2</sub>, Al<sub>2</sub>O<sub>3</sub>, CaO and MgO are 5.92%, 1.98%, 0.47% and 0.36%, respectively. The particle size of pyrite cinder can be found in Table 2. The analytical reagent of borax (Na<sub>2</sub>B<sub>4</sub>O<sub>7</sub>·10H<sub>2</sub>O) was used during the experiment.

**Table 1.** Chemical composition of pyrite cinder (mass/%). TFe: Total Fe; LOI: Loss of ignition.

Element	TFe	FeO	SiO <sub>2</sub>	Al <sub>2</sub> O <sub>3</sub>	CaO	MgO	K <sub>2</sub> O	Na <sub>2</sub> O	P	S	LOI
Content	60.95	12.61	5.92	1.98	0.47	0.36	0.21	0.05	0.04	0.39	1.12

**Table 2.** Particle size of pyrite cinder (mass/%).

Size	0.15–0.106 mm	0.106–0.074 mm	0.074–0.044 mm	–0.044 mm
Content	6.47	14.97	19.85	58.71

Bituminous coal was used as a reductant. The industrial analysis results and particle size are given in Tables 3 and 4. The fixed carbon is 50.04%, volatile is 30.15% and ash content is 12.04%, which is suitable for the reduction [13]. The particle size of bituminous coal is 100% passing through 5 mm and 75.52% passing through 0.5 mm.

**Table 3.** Industrial analysis results of bituminous coal (mass/%).

Item	Fixed Carbon	Moisture	Ash	Volatiles	Sulfur
Content	50.04	7.97	12.04	30.15	0.37

**Table 4.** Particle size of bituminous coal (mass/%).

Size	5–1 mm	1–0.5 mm	0.5–0 mm
Content	58.29	17.23	24.48

### 2.2. Methods

#### 2.2.1. Reduction Roasting and Magnetic Separation

The main process of the experiment contains five steps, which are briquetting, pre-oxidizing, reduction, ball-milling and magnetic separation. Firstly, the pyrite cinder and borax additives were mixed to prepare the briquettes. The briquettes were made by pressing the material mixture in a cylindrical mould for 1 min under the pressure of 8 MPa. The briquettes made are 10 mm in diameter and 15 mm in height. The drying of the briquettes was carried out in the oven at 105 °C for 4 h.

The pre-oxidization of pyrite cinder briquettes was carried out in a tube furnace (Φ 50 × 600 mm, Brother company, Zhengzhou, China). The briquettes were loaded in a porcelain boat crucible of 60 mm in length and 30 mm in width. Then the porcelain boat was put into the central area of the tube furnace and oxidized at 1050 °C for 10 min.

After the pre-oxidization, the pre-oxidized briquettes were reduced in a shaft furnace (Φ 80 × 800 mm, Brother company, Zhengzhou, China). The graphite crucible of 60 mm in diameter and 150 mm in height, containing 30 g pre-oxidized briquettes and 60 g reductant, was put into the shaft furnace after the target temperature was reached. The upper end of corundum tube was covered with a refractory block during reduction in order to maintain enough CO concentration in the shaft

furnace. After the reduction, nitrogen with a flow rate of 1 L/min was introduced to the crucible to cool down to prevent deoxidizing. Through that, the reduced pyrite cinder briquettes were obtained.

The magnetic separation was performed in the magnetic tube after the reduced briquettes were ground in the cone ball mill. The final metallic iron powder was obtained after magnetic separation at the magnetic intensity of 0.08 T. The model of the cone ball mill is XMQ240 × 90 (Luoke company, Wuhan, China) and the laboratory magnetic equipment is a Davis tube of XCGS-73 (Shunze company, Changsha, China).

### 2.2.2. Methods of Analysis

The chemical compositions of samples and the final product were obtained from ICP-MS (inductively coupled plasma mass spectrometry, Thermo Electron corporation, Waltham, MA, America). The crystalline phase of the samples was investigated by the XRD technique, and the structures and element distribution of the reduced briquettes were analyzed by scanning electron microscope (SEM) (Oxford, UK) with energy dispersion system (EDS) (Oxford, UK).

The total iron (TFe, wt. %) content and metallic iron (MFe, wt. %) content in the iron concentrate (metallic iron powder) were obtained by chemical methods, and the metallization degree,  $\eta$ , was calculated by

$$\eta = \frac{\text{MFe}}{\text{TFe}} \times 100\% \quad (1)$$

The iron recovery,  $\varepsilon$ , was calculated by the following formula:

$$\varepsilon = \gamma \times \frac{\beta}{\alpha} \quad (2)$$

where  $\gamma$  is the yield of iron concentrate during the magnetic separation, wt. %;  $\beta$  is the Fe content of the iron concentrate, wt. %;  $\alpha$  is the Fe content of the reduced briquettes, wt. %.

## 3. Results and Discussion

### 3.1. Effect of Borax Additive Dosage

The effects of the dosage of borax on the iron grade of the magnetic concentrate, iron recovery and metallization degree of the reduced briquettes were investigated, which was shown in Figure 1. With the increase of the borax dosage, the iron grade of the magnetic concentrate increases, but the iron recovery decreases (Figure 1a). It is mainly because the borax can enhance the lattice defect of the iron ore [14]. During the pre-oxidization, the borax can improve the re-crystallization of the iron oxide crystal grains and therefore enlarge the iron oxide particles [15]. On the other hand, borax also creates more lattice defects of metallic iron to improve the re-crystallization of the metallic iron crystal grains, which leads to the growth and interconnection of iron particles (Figures 2 and 3). The remarkable interconnection and growth of iron particles promote the dissociation of iron and gangue, so the iron grade goes up. As the interconnection and growth of iron particles cause weak diffusion of CO in the briquettes, it imposes a negative influence on the metallization degree (Figure 1b). The low metallization degree results in the decrease in the iron recovery rate (Figure 1b). When the dosage of the borax exceeds 5%, the iron grade of the magnetic concentrate declines. It can be explained by the fact that the borax is liquid during the test temperature range, and the amount of liquid borax limits the interconnection and growth of iron particles (Figure 2), which leads to the decrease of the iron grade of the magnetic concentrate.

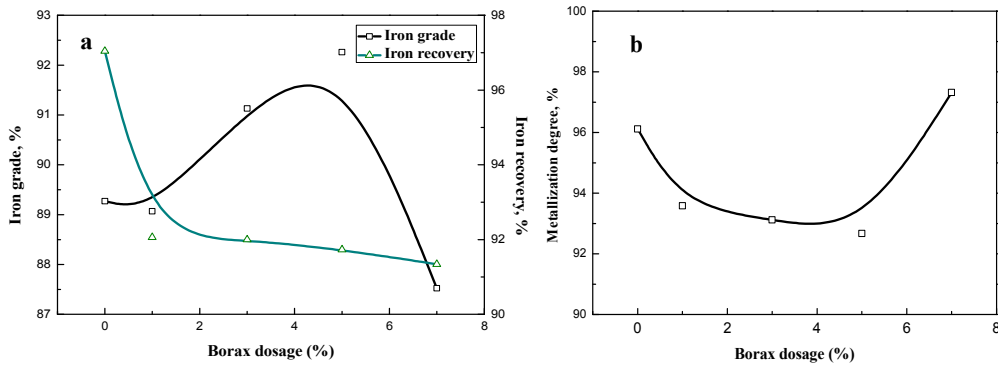


**Figure 1.** Effect of borax dosage on iron grade and iron recovery of magnetic concentrate (a); and effect of borax dosage on metallization degree of reduced briquettes (b) (reducing at 1050 °C for 80 min, and grinding fineness (<0.044 mm) exceeding 68%).

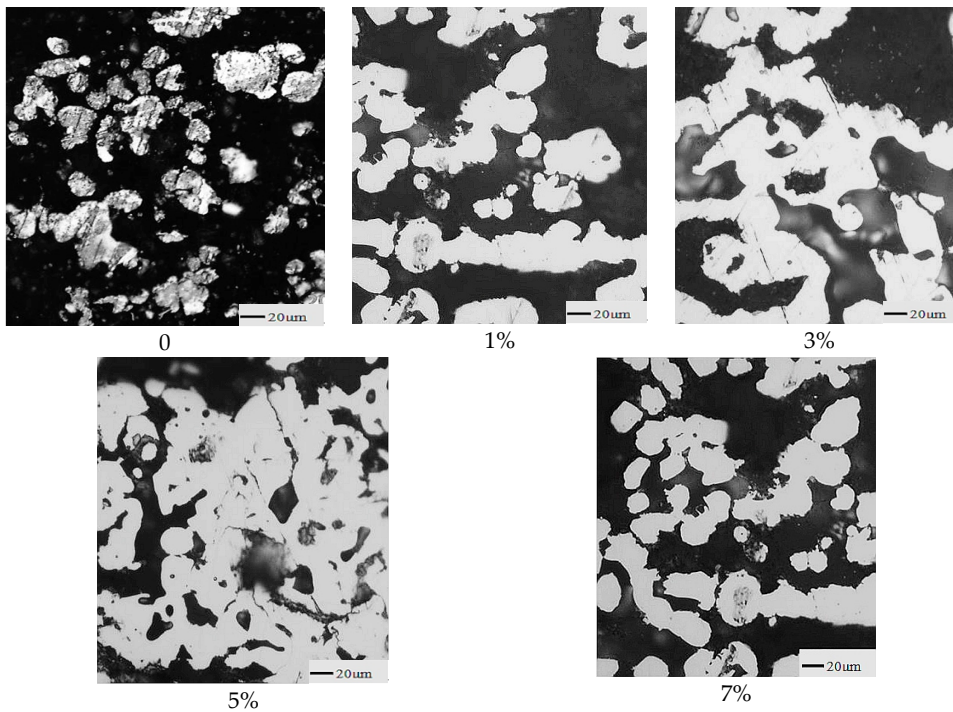


**Figure 2.** Microstructure of reduced briquettes with different dosage of borax (bright white, metallic iron).

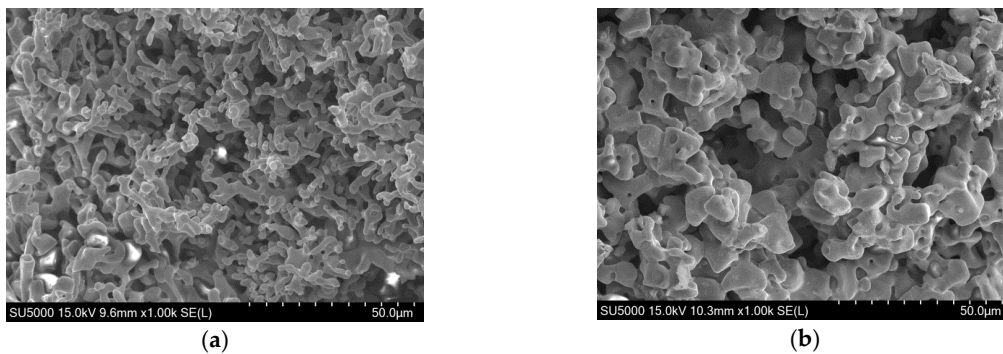


**Figure 3.** Microstructure of reduced briquettes with different dosage of borax by scanning electron microscope (SEM) ((a): 0% borax; (b): 5% borax).

### 3.2. Effect of Reduction Temperature

The effect of the reduction temperature on the metallization degree of the reduced briquettes, iron grade and iron recovery of the magnetic concentrate are shown in Figure 4. It is clear that the iron grade of the magnetic concentrate and the recovery rate of iron both increase with the increase in temperature, especially the iron recovery (Figure 4a). The reason is that the Boudouard reaction is very active at high temperatures, which improves the metallization degree of the reduced briquettes (Figure 4b). Furthermore, a high reduction temperature accelerates the re-crystallization of the crystal grains of metallic iron. The particle size of metallic iron is larger at higher temperatures (Figure 5), so the dissociation of iron and gangue becomes easier.

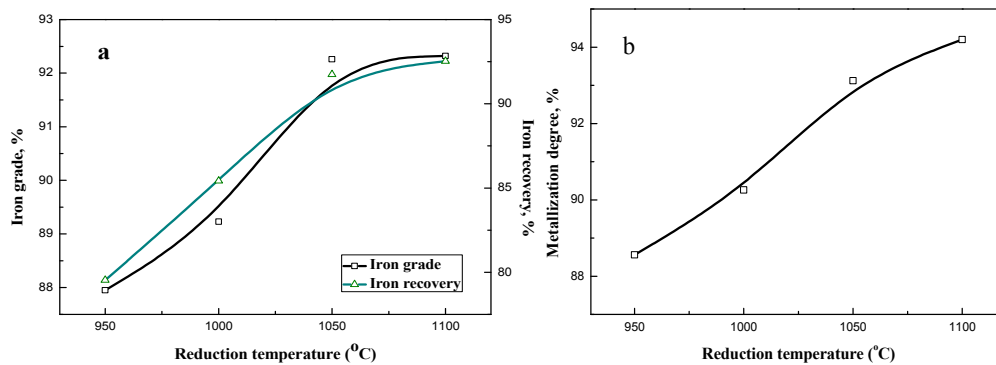


**Figure 4.** Effect of reduction temperature on iron grade and iron recovery of magnetic concentrate (a); and effect of reduction temperature on metallization degree of reduced briquettes (b) (borax dosage of 5%, reducing for 80 min, and grinding fineness (<0.044 mm) exceeding 68%).

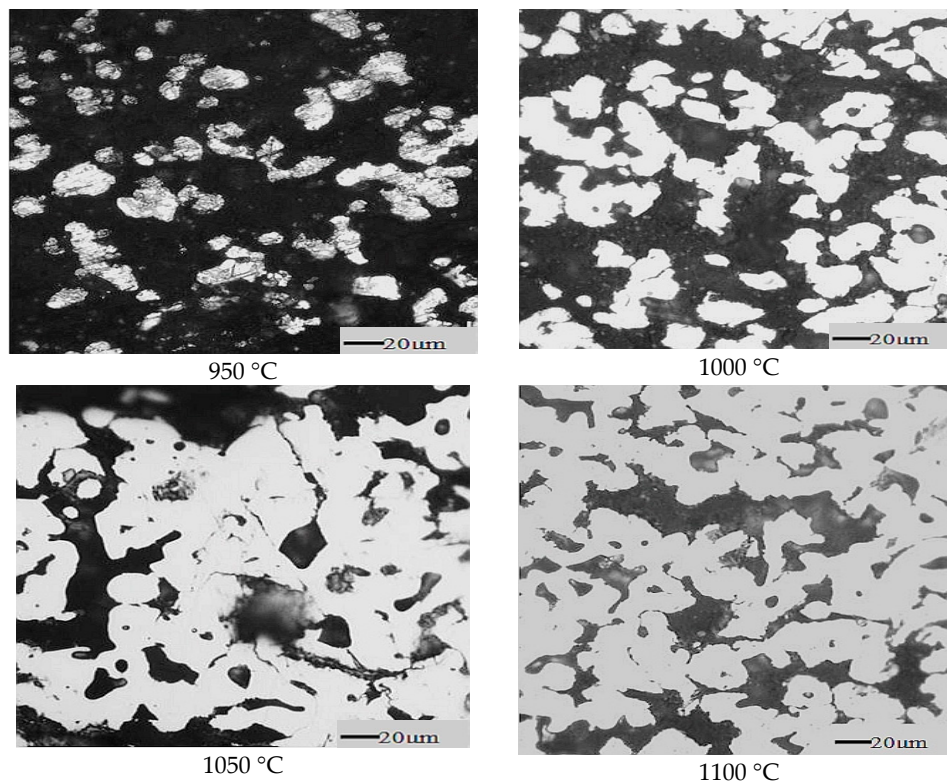


**Figure 5.** Microstructure of reduced briquettes at different reduction temperature (bright white, metallic iron).

### 3.3. Effect of Reduction Time

Figure 6 displays the influence of reduction time on the metallization degree of the reduced briquettes, iron grade and iron recovery of the magnetic concentrate. The metallization degree of the reduced briquettes significantly rises with the prolonged reduction time (Figure 6a), so both the iron grade and iron recovery of the magnetic concentrate increase (Figure 6b). Also, the particle size of metallic iron has a clear uptrend with a long reduction time [16].

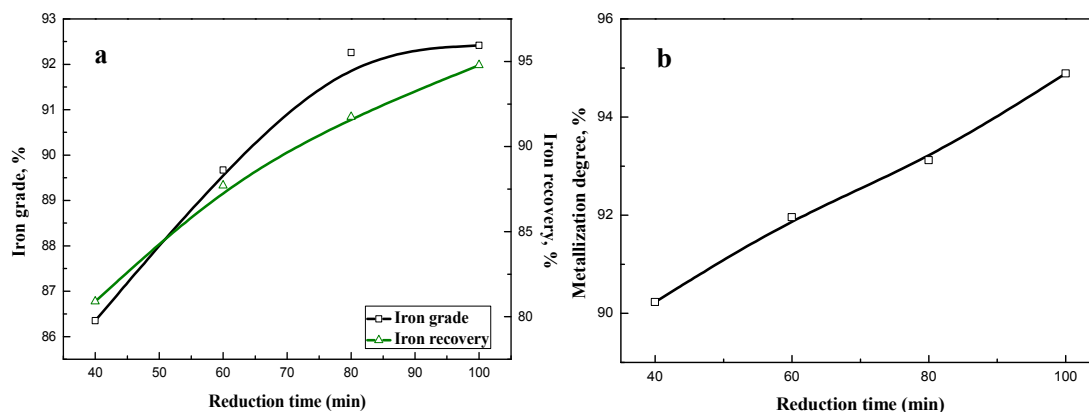


**Figure 6.** Effect of reduction time on iron grade and iron recovery of magnetic concentrate (a); and effect of reduction time on metallization degree of reduced briquettes (b) (borax dosage of 5%, reducing at 1050 °C, and grinding fineness (<0.044 mm) exceeding 68%).

### 3.4. Effect of Grinding Fineness

Figure 7 shows the effect of grinding fineness on the iron grade and iron recovery of the magnetic concentrate. It illustrates that the recovery rate of the magnetic concentrate drops with the increase of grinding fineness. The iron grade of the magnetic concentrate was promoted. All these can be explained by the fact that when the grinding particle is fine, the dissociation degree of the iron particles of metallic iron and the gangue particles is enhanced. When the grinding fineness (<44  $\mu\text{m}$ ) exceeds 81%, there is a drop in the iron grade of the magnetic concentrate. This is because the iron ore and gangue irons are completely mixed when the grinding particle is too fine, which weakens the separation efficiency of the iron and gangue.

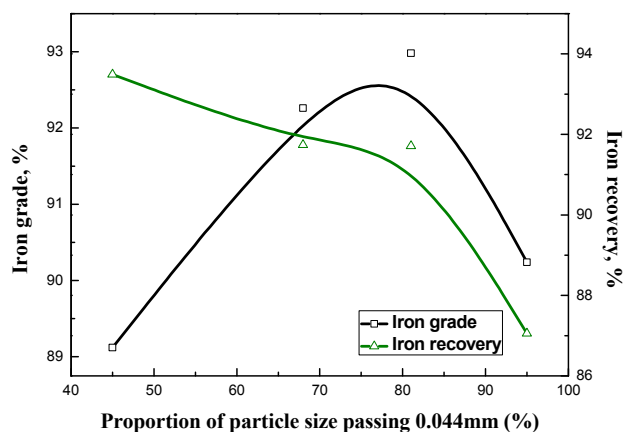


**Figure 7.** Effect of grinding fineness on iron grade and iron recovery of magnetic concentrate (borax dosage of 5%, and reducing at 1050 °C for 80 min).

### 3.5. Analysis of the Final Product

The magnetic concentrates achieved were analyzed by XRD and SEM-EDS. XRD patterns of the magnetic concentrate and pyrite cinder are displayed in Figure 8. The iron of the pyrite cinder before pre-oxidization is mainly in the form of magnetite, hematite and maghemite, and the gangue is in the form of quartzes. After the reduction, ball milling and magnetic separation, the magnetic concentration prepared mostly presents in metallic phase, and no gangue phase exists. Thus, the dissociation of iron and gangue executes well.

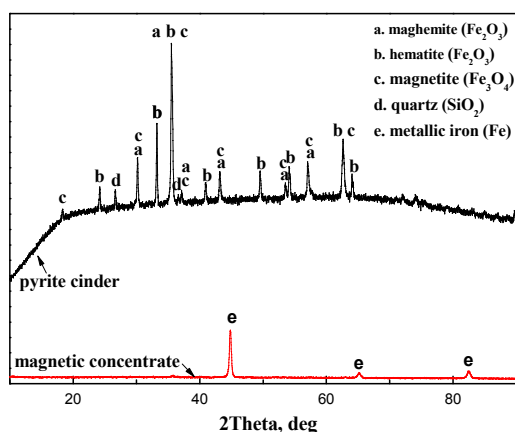


**Figure 8.** X-ray diffraction (XRD) patterns of magnetic concentrate and pyrite cinder (borax dosage of 5%, reducing at 1050 °C for 80 min, and grinding fineness (<0.044 mm) exceeding 81%).

SEM-EDS of the magnetic concentrate under the optimum condition is shown in Figure 9. The particles of the magnetic concentration are mainly in the shape of flakes due to good ductility of the metallic iron. As shown in Figure 9, the particles such as point A are mainly in metallic iron phases. The particles such as point B are the gangue and some iron minerals. The gangue particle in the magnetic concentrate is embedded in the particle of the metallic iron, which indicates it is very difficult to remove the residual gangue in magnetic concentrate.

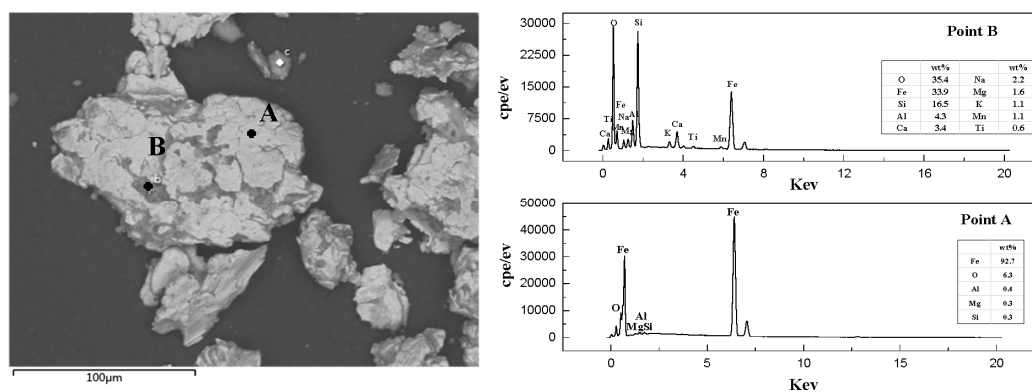


**Figure 9.** Scanning electron microscope with energy dispersion system (SEM-EDS) of the magnetic concentrate under the optimum condition (borax dosage of 5%, reducing at 1050 °C for 80 min, and grinding fineness (<0.044 mm) exceeding 81%).

Compared with the traditional recovery of iron from iron ores, the operation cost of adding a borax reduction roasting to treat the pyrite cinder is high, but the technology of adding borax roasting and magnetic separation opens the way to recover iron from the pyrite cinder [17–19].

#### 4. Conclusions

Reduction roasting and magnetic separation is one of the efficient ways to retrieve the metallic iron powder from pyrite cinder, and borax is an effective additive to improve the separation efficiency of the iron and gangue of the pyrite cinder. During the reduction process, borax can significantly promote the particle size of the metallic iron, which further improves the separation of the iron particles and gangue and increases the iron grade of the magnetic concentration. The final product, assaying 92.98% TFe with the recovery of 91.71%, was obtained under the optimum conditions, which can be used as the burden for steel-making instead of parts of scrap.

**Acknowledgments:** The authors are thankful to the projects by National Natural Science Fund China (51504003) and Science and Technology Development Anhui Province (1501041126) and National Natural Science Fund Anhui Province (1608085QE94) and the Key Project of Natural Science Research of Anhui Universities (KJ2015A028) for sponsoring the research work.

**Author Contributions:** Hongming Long and Jiaxin Li conceived and designed the experiments; Qingmin Meng performed the experiments; Ping Wang and Zhanxia Di analyzed the data; Qingmin Meng contributed reagents, materials, and analysis tools; Tiejun Chun wrote the paper.

**Conflicts of Interest:** The authors declare no conflict of interest.

#### References

1. Zhu, D.Q.; Chun, T.J.; Pan, J.; Guo, Z.Q. Preparation of oxidised pellets using pyrite cinders as raw material. *Ironmak. Steelmak.* **2013**, *40*, 430–435. [[CrossRef](#)]
2. Zheng, Y.; Liu, Z. Preparation of monodispersed micaceous iron oxide pigment from pyrite cinders. *Powder Technol.* **2011**, *207*, 335–342. [[CrossRef](#)]
3. Giunti, M.; Baroni, D.; Bacci, E. Hazard assessment to workers of trace metal content in pyrite cinders. *Bull. Environ. Contamin. Toxicol.* **2004**, *72*, 352–357. [[CrossRef](#)] [[PubMed](#)]
4. Ye, Z.P.; He, G.W. Research on recycling technology and waste water treatment with sulfuric acid residue. *J. South China Norm. Univ.* **2010**, *2*, 72–75. (In Chinese)
5. Jin, C.; Li, D.X. Research progress on the comprehensive utilization of iron from pyrite cinder. *Metal Mine* **2011**, *10*, 162–165.
6. Bi, W.L.; Wu, W.H.; Li, J. Experimental research on recovering of iron concentrate from pyrite cinder. *Hydrometall. China* **2011**, *30*, 229–230. (In Chinese)
7. Wang, Q.L.; Zhou, H.Q.; Dai, Y.H. Technological research on desulfurizing flotation of pyrite cinder in Guangxi. *Min. Metal. Eng.* **2008**, *28*, 44–46.
8. Zheng, Z.F.; Li, M.L. Experimental study on iron recovery from pyrite cinder. *Min. Metal. Eng.* **2006**, *26*, 29–32.
9. He, B.; Tian, X.; Sun, Y.; Yang, C.; Zeng, Y.; Wang, Y.; Zhang, S.; Pi, Z. Recovery of iron oxide concentrate from high-sulfur and low-grade pyrite cinder using an innovative beneficiating process. *Hydrometallurgy* **2010**, *104*, 241–246. [[CrossRef](#)]
10. Jin, C.; Wang, E.Q.; Li, D.X. Pressure reduction leaching iron from sulfate slag. *Nonferr. Metals* **2011**, *11*, 6–8.
11. Long, H.M.; Meng, Q.M.; Wang, P.; Chun, T.J.; Yao, Y.L. Preparation of chromium-iron metal powder from chromium slag by reduction roasting and magnetic separation. *J. IronSteel Res. Int.* **2015**, *22*, 771–776. [[CrossRef](#)]
12. Chun, T.J.; Long, H.M.; Li, J.X. Alumina-iron separation of high alumina iron ore by carbothermic reduction and Magnetic separation. *Separat. Sci. Technol.* **2015**, *50*, 760–766. [[CrossRef](#)]
13. Qiu, G.Z.; Jiang, T.; Xu, T.J.; Cai, R.Z. *Direct Reduction of Cold-bonded Pellets*; Centre South University Press: Changsha, China, 2001; pp. 176–180.
14. Zhu, D.Q.; Zhou, W.T.; Pan, J.; Chen, D. Improving pelletization of Brazilian hematite by adding boron-containing magnetite. *J. Cent. South Univ. Sci. Technol.* **2014**, *45*, 348–355. (In Chinese)
15. Chun, T.J.; Zhu, D.Q.; Pan, J.; He, Z. Preparation of metallic iron powder from red mud by sodium salt roasting and magnetic separation. *Can. Metal. Q.* **2014**, *53*, 183–189. [[CrossRef](#)]



16. Chen, D.; Zhu, D.Q.; Chen, Y. Preparation of prereduced pellets by pyrite cinder containing nonferrous metals with high temperature chloridizing-reduction roasting technology. *ISIJ Int.* **2014**, *54*, 2162–2168. [[CrossRef](#)]
17. Zhang, K.; Nieto, A.; Kleit, A. Valuation of mining operation with uncertainty and the power of waiting—A real option method. In *Mine Planning and Equipment Selection*; Springer publisher: Berlin, Germany, 2014; pp. 1503–1512.
18. Zhang, K.; Kleit, A.N. Mining rate optimization considering the stockpiling: A theoretical economics and real option model. *Resour. Policy* **2016**, *31*, 87–94. [[CrossRef](#)]
19. Chun, T.J.; Zhu, D.Q.; Pan, J. Simultaneously roasting and magnetic separation to treat low grade siderite and hematite ores. *Miner. Process. Extr. Metal. Rev.* **2015**, *36*, 223–226. [[CrossRef](#)]



© 2016 by the authors; licensee MDPI, Basel, Switzerland. This article is an open access article distributed under the terms and conditions of the Creative Commons Attribution (CC-BY) license (<http://creativecommons.org/licenses/by/4.0/>).